Development of a method for the measurement of long-range ^{13}C–^{1}H coupling constants from HMBC spectra

Richard A E Edden and James Keeler *

University of Cambridge, Department of Chemistry, Lensfield Rd, Cambridge, CB2 1EW, U.K.

Abstract

This paper describes a number of improvements to a method, developed in this laboratory and described in *J. Magn. Reson.* **85** (1989) 111-113, which makes it possible to determine values of long-range ^{13}C–^{1}H coupling constants from HMBC spectra. Firstly, it is shown how pulsed-field gradients can be introduced into the HMBC experiment without perturbing the form of the cross-peak multiplets; a one-dimensional version of the experiment is also described which permits the rapid measurement of a small number of couplings. Secondly, the experiment is modified so that one-bond and long-range cross peaks can be separated, and so that the one-bond cross peaks have more reliable intensities. Finally, it is shown how these one-bond cross peaks can be used to advantage in the fitting procedure.

Key words: HMBC, long-range C–H coupling, fitting, MBOB
PACS:

1 Introduction

The HMBC (heteronuclear multiple bond correlation) [1] experiment has become the standard way of detecting the presence of long-range ^{13}C–^{1}H couplings in small- to medium-sized molecules. However, from such a spectrum it is not at all straightforward to determine the numerical value of the coupling constant. The difficulty derives from the fact that the multiplets in the proton (F_2) dimension have complex phase properties due to the evolution of

---

* Corresponding author
    Email address: James.Keeler@ch.cam.ac.uk (James Keeler).
    URL: www-keeler.ch.cam.ac.uk (James Keeler).

proton–proton couplings and proton chemical shifts (offsets); in addition, the long-range coupling appears as an anti-phase splitting. It is thus not possible to identify, from the multiplet, a splitting which corresponds to the value of the long-range coupling constant.

Previous work from this laboratory [2] introduced a fitting procedure which makes it possible to determine a value for the long-range coupling constant from an HMBC multiplet. The procedure works by comparing the HMBC multiplet with the corresponding multiplet from a conventional proton spectrum (called the *template*); a least-squares fitting procedure, involving just two parameters, yields a value for the long-range C–H coupling. If the conventional proton spectrum is crowded, the proton multiplets needed for the fitting procedure can be obtained from two-dimensional spectra provided that the multiplets are in-phase and otherwise undistorted. For example, such multiplets can be obtained from TOCSY spectra [3] in which the anti-phase dispersive contributions have been suppressed effectively [4].

In this paper we describe a number of developments of this basic approach. Firstly, the HMBC experiment is updated by the use of gradient pulses so that high-quality data can be obtained; we also discuss the problem of phasing such spectra. Secondly, an experimental approach is described which makes it possible to obtain, from one set of experimental data, both the HMBC spectrum and a complete one-bond correlation spectrum from which templates can be obtained. Obtaining the templates in this way is convenient as, compared to the conventional proton spectrum, the likelihood of overlap is reduced. We also introduce a new way in which these one-bond cross peaks can be used in the fitting procedure. The utility of the whole approach is illustrated by measuring the values of numerous long-range couplings in strychnine.

Finally, we introduce a one-dimensional version of the HMBC experiment which results in multiplets that can be analysed in the same way as those from the two-dimensional experiments. In cases where only a few couplings are of interest, a selective experiment such as this may be an attractive alternative to recording a two-dimensional experiment.

The fitting procedure itself is not computationally demanding and can be implemented on a desk-top computer. A program, designed to work within Bruker's XWIN-NMR$^{©}$ and available without charge from the authors' web site, has been developed to carry out the fitting procedure.

2 The basic HMBC experiment and fitting procedure

The way in which the fitting procedure works and the required modifications to the HMBC experiment have been described in the earlier work from this laboratory [2]. However, it is useful to repeat these here as they form the basis for the description of subsequent modifications, which are the topic of this paper.

[Fig. 1 about here.]

The pulse sequence for the basic HMBC experiment is shown in Fig. 1 (a). Proton magnetization excited by the first pulse evolves during the *preparation delay*, Δ, to become anti-phase with respect to the long-range C–H coupling; this anti-phase magnetization is converted into heteronuclear multiple quantum coherence by the first ^{13}C pulse. The coherence evolves for time t_1 during which it acquires a phase label according to the ^{13}C offset; the evolution of the proton offset during t_1 is refocused by the centrally-placed 180° pulse on proton. Finally, the second ^{13}C pulse returns the multiple quantum coherence to proton magnetization which is anti-phase with respect to the (active) long-range C–H coupling.

Although the proton 180° pulse refocuses the evolution of the proton offset over the time t_1, both the offset and any proton–proton couplings evolve throughout the delay Δ, thus giving rise to a phase modulation of the observed signal. As Δ has to be comparable with $1/(2\ ^{n}J_{\mathrm{CH}})$, the evolution of any proton-proton couplings present is certainly significant. It is this modulation, combined with the presence of the anti-phase splitting with respect to the C–H coupling, that gives the HMBC multiplet its complex phase properties.

For the fitting procedure to work correctly, it is essential that the phase modulation in the HMBC experiment is *identical* to that which would arise from a simple delay Δ. In the basic HMBC experiment this is *not* the case, due to the the presence of the proton 180° pulse. However, the required phase modulation can be achieved by adding a second proton 180° pulse at the end of t_1, as shown in Fig. 1(a). This extra pulse effectively restricts the refocusing effect of the first 180° pulse to the t_1 period. From now on we will assume that it is this slightly modified form of the HMBC experiment which is being discussed.

The HMBC spectrum is invariant to the sign of the C–H coupling, so the fitting procedure can give no information in this regard. Therefore, throughout this work we are only able to quote the magnitude of the coupling constant.

2.1 The fitting procedure (Method I)

The way in which the fitting procedure works is best envisaged in the time domain. If we imagine taking a cross-section parallel to F_2 (the proton dimension) through a cross peak in an HMBC spectrum, the time-domain signal corresponding to the cross peak can be written as

$$S_{\text{HMBC}}(t_2) = A_{\text{HMBC}} \times S_{\text{proton}}(t_2 + \Delta) \times \sin{(\pi J_{\text{CH}} t_2)} \tag{1}$$

where J_{CH} is the long-range coupling responsible for the cross peak and A_{HMBC} is the overall amplitude; the factor $\sin{(\pi J_{\text{CH}} \Delta)}$, which describes the dependence of the amplitude of the cross peak on the preparation delay, is included in A_{HMBC}. In Eq. 1 the term $\sin{(\pi J_{\text{CH}} t_2)}$ results in the observed multiplet being anti-phase with respect to the active coupling J_{CH}.

S_{proton} is the time-domain signal corresponding to the normal proton multiplet, with no C–H coupling present, such as would be acquired in a conventional pulse–acquire experiment. This signal can be written as:

$$S_{\text{proton}}(t_2) = \exp{(i\Omega_{\text{H}_1} t_2)} \times \prod_i \cos{(\pi J_{\text{H}_1 \text{H}_i} t_2)} \tag{2}$$

where Ω_{H_1} is the offset of the proton involved in the cross peak (proton 1) and $J_{\text{H}_1 \text{H}_i}$ is the coupling of proton 1 to proton i. The product of cosine terms simply expresses, in the time domain, the successive in-phase splittings that each of these couplings causes. Note that, in contrast to the anti-phase C–H coupling, these in-phase H–H couplings are represented by cosine terms.

In the expression for $S_{\text{HMBC}}(t_2)$, Eq. 1, the term $S_{\text{proton}}(t_2 + \Delta)$ shows that at the start of acquisition (i.e. $t_2 = 0$) there has already been evolution of the proton offset and proton–proton couplings for time Δ.

The basis of our fitting method is the observation that the phase modulation due to the evolution of the proton offset and proton-proton couplings during delay Δ in the HMBC experiment is *identical* in form to that found for the simple $90°$–Δ–acquire(t_2) sequence. The signal from this experiment can be written

$$S_{\text{1D}}(t_2) = S_{\text{proton}}(t_2 + \Delta). \tag{3}$$

The only differences between $S_{\text{1D}}(t_2)$ and the signal from the HMBC cross peak ($S_{\text{HMBC}}(t_2)$ of Eq. 1) are the amplitude and the presence of the sine term in the latter.

4

The fitting procedure involves forming a *trial multiplet* by multiplying the time-domain signal for the phase-modulated proton multiplet, $S_{1D}(t_2)$ of Eq. 3, by a trial amplitude, A_{trial}, and a sine term to create an anti-phase splitting, $\sin(\pi J_{trial}t_2)$:

$$
\begin{aligned}
S_{trial}(t_2) &= A_{trial} \times S_{1D}(t_2) \times \sin(\pi J_{trial}t_2) \\
&= A_{trial} \times S_{proton}(t_2 + \Delta) \times \sin(\pi J_{trial}t_2).
\end{aligned}
\tag{4}
$$

We see that, provided $A_{trial} = A_{HMBC}$ and $J_{trial} = J_{CH}$, $S_{trial}(t_2)$ becomes identical to $S_{HMBC}(t_2)$ of Eq. 1. This, then, is the basis of a fitting procedure in which A_{trial} and J_{trial} are varied until $S_{trial}(t_2)$ and $S_{HMBC}(t_2)$ match as closely as possible. This is achieved by minimizing the following χ^2 function:

$$
\chi^2 = \int_0^{t_{2,max}} |S_{trial}(t_2) - S_{HMBC}(t_2)|^2 \, dt_2.
\tag{5}
$$

In Eq. 5 we have allowed for the fact that the signals are complex. For convenience we refer to this original version of the fitting procedure as *Method I*.

[Fig. 2 about here.]

It is convenient to perform the fitting routine in the time domain, but the whole process can just as well be envisaged in the frequency domain; Fig. 2 illustrates the fitting process in the two domains.

The form of the phase modulation due to proton offsets and proton–proton couplings is only the same in the 90°–Δ–acquire(t_2) and HMBC experiments if the modified HMBC experiment of Fig. 1 (a) is used. It is not actually necessary to record the 90°–Δ–acquire(t_2) experiment. Rather, we simply record a conventional proton spectrum and then left shift the time-domain signal by a number of data points corresponding to the time Δ.

It is important to make sure that, for both the HMBC spectrum and the normal proton spectrum, we deal with a single multiplet. This is achieved by excising the relevant multiplet from a one-dimensional spectrum or cross section through a two-dimensional spectrum, by setting to zero all of the data points which do not define the multiplet. Having done this, the spectrum is inverse Fourier transformed to generate the time-domain signal, $S_{HMBC}(t_2)$ or $S_{proton}(t_2)$. Only then is the left shift applied to $S_{proton}(t_2)$ in order to create the phase modulation.

As an absorption mode spectrum has the best resolution, it is usual to phase the proton spectrum to absorption before the wanted multiplet is excised.

However, although the real part of the (phased) spectrum is in the absorption mode, the imaginary part will contain the much broader dispersion mode multiplet. To get around this problem we excise the absorption mode multiplet from the real part of the spectrum and then generate the corresponding imaginary part using a Hilbert transform; further details can be found in reference [5]. The resulting complex frequency-domain signal can then be inverse Fourier transformed to give the required time-domain signal.

3 Introducing gradients into the HMBC experiment

For the fitting procedure to work as planned, it is clearly important that the HMBC spectra are of the highest quality. The use of pulsed field gradients for coherence selection is therefore to be recommended, as it is known that spectra recorded in this way are generally superior to those recorded using phase cycling.

There are many different ways in which gradients can be implemented into the HMBC experiment, but for the fitting procedure described in the previous section to be applicable, we have to be careful to ensure that the resulting multiplets have exactly the same phase properties as those obtained from the sequence of Fig. 1(a).

One implementation which satisfies these requirements, and which we have found to yield good spectra, is shown in Fig. 1(b). This sequence is the same as that proposed by Cicero et al. [6] but with the addition of an extra 180° pulse on proton at the end of t_1. As with sequence (a), this extra pulse is needed so as to ensure that the proton evolution is identical to that of the simple 90°–Δ–acquire(t_2) experiment. In fact, because of the extra delays δ needed to accommodate the gradients, the proton offsets and couplings evolve for a time $(\Delta + 2\delta)$; this total delay must be used when constructing the trial multiplet.

The 180° pulse on carbon allows selection of the required coherence order by the two gradients G_1 and G_2; this pulse also refocuses any evolution of the carbon offset which takes place during the two gradients. The gradient ratio, G_1/G_2, is set to $-4.975/2.975$ to record N-type data and $-2.975/4.975$ to record P-type data. These two data sets are subsequently recombined in the usual way to give a frequency-discriminated, absorption mode spectrum [7].

3.1 Phase correction

The presence during t_1 of several pulses of finite duration makes it impossible to acquire data for $t_1 = 0$, leading to large frequency-dependent phase errors in the F_1 (carbon) dimension. While these can, in principle, be removed by manual phasing in the usual way, such large linear phase corrections tend to resulted in distorted baselines. However, Zhu et al. [8] have shown that if the phase error across the spectrum is 180° or 360°, subsequent correction does not lead to such baseline distortions. Thus, all that is required is that the initial value of t_1 be chosen to achieve such a phase error of 180° or 360°.

Referring to Fig. 1 (b), the delays during which the carbon offset evolves can be identified as: the first period $t_1/2$, the duration of the first proton 180° pulse, the second period $t_1/2$, and the duration of the second proton 180° pulse. The evolution over the two delays δ is, to a good approximation, refocused by the carbon 180° pulse.

Suppose that the initial value set for the delay $t_1/2$ is $t_{1,\mathrm{min}}/2$. Then, for the first increment of the two-dimensional experiment, the time for which the carbon offset evolves, $t_1^{(0)}$, is

$$t_1^{(0)} = 2 \times (t_{1,\mathrm{min}}/2) + 2 \times t_{180}, \tag{6}$$

where t_{180} is the duration of the 180° pulses. Zhu et al. show that a linear phase correction of $(n \times 180°)$ (where n is an integer) will be obtained if $t_1^{(0)}$ satisfies

$$t_1^{(0)} = \frac{n}{2} \, \delta_1, \tag{7}$$

where δ_1 is the increment of t_1, set by the required spectral width in F_1. In practice, $t_{1,\mathrm{min}}/2$ is chosen so that Eq. 7 is satisfied. Finally, it should be noted that as the time point $t_1 = 0$ is not being sampled, it is not necessary to halve the value of the first data point.

For example, in the experiments reported below the F_1 spectral width of 181 ppm (22624 Hz at a proton frequency of 500 MHz) gives a t_1 increment, δ_1, of 44.2 μs. The 180° pulse-length, t_{180}, was 22.0 μs, so Eq. 7 can be satisfied for $n = 2$ by choosing $t_{1,\mathrm{min}}/2 = 0.1$ μs.

In F_2 there is, in general, no phase correction which will result in absorption mode multiplets; phase correction is, therefore, superfluous. However, it is desirable to phase the proton spectrum from which the templates are to be taken so as to minimize the overlap between multiplets. If this is done, it is

essential to apply the *same* correction to the HMBC spectrum so that the multiplets are comparable. An alternative, which we have found convenient, is leave the HMBC spectra unaltered and to simply "undo" the phase correction of the proton spectrum by applying to the template the opposite of the original phase correction *after* the multiplet has been excised.

There is one further matter to take into account in respect of the phase in F_2. This is the fact that, all other things being equal, there is a 90° phase difference between the peaks in the HMBC and in the proton spectrum. In the simple proton experiment it is the in-phase magnetization which is the origin of the observed signal. In contrast, in the HMBC experiment, the proton magnetization which is anti-phase with respect to the ^{13}C ultimately leads to the observed signal. The evolution of in-phase magnetization (e.g. I_{1y}) to anti-phase magnetization (e.g. $2I_{1x}S_z$) involves a shift from the y- to the x-axis; this is the origin of the 90° phase shift between the two spectra. In practice, this phase shift is accounted for by multiplying the trial multiplet by $\exp(i\pi/2) = i$ prior to the fitting i.e. A_{trial} should be purely imaginary.

[Fig. 3 about here.]

Figure 4 shows the result of the fitting procedure applied to the C8–H13 cross-peak multiplet from strychnine (structure and numbering shown in Fig. 3). With the correct choice of the two parameters, there is clearly an excellent fit between the trial multiplet and the multiplet from the HMBC. The contour plot of χ^2, as defined in Eq. 5, as a function of the two parameters shows that the minimum is well defined so that it can easily be located by a simple search program, such as the standard Levenberg–Marquardt algorithm [9].

[Fig. 4 about here.]

Typically, we construct this contour plot using quite a coarse grid of values for the two parameters. This enables us to identify the approximate position of the minimum, and then the values of the parameters at this point are used as starting values for the Levenberg–Marquardt algorithm. Usually, this leads to swift convergence.

The two modified versions of the fitting procedure described below involve further parameters, so it is not easy to visualize how χ^2 depends on their values. In such cases we use the best estimates we can for these additional parameters and then plot how χ^2 depends on J_{trial} and A_{trial}. The position of the minimum identified in such a plot is used to obtain starting values for the Levenberg–Marquardt algorithm which is then allowed to alter the values of *all* of the parameters. When using this approach, the minimum located by the Levenberg–Marquardt algorithm may deviate somewhat from that seen in the initial χ^2 contour plot.

4   Using one-bond cross peaks as templates

It is often the case that cross peaks arising from one-bond C–H correlations appear in HMBC spectra. These one-bond cross peaks have identical structure to the long-range cross peaks i.e. both are phase modulated by proton offsets and couplings, and anti-phase with respect to the C–H coupling. However, as the one-bond coupling is much larger than the width of the proton multiplet, the one-bond and long-range cross peaks look rather different. For the one-bond cross peak we see two clearly separated proton multiplets, separated by the one-bond coupling and disposed symmetrically about the proton offset. In contrast, the long-range cross peak appears as a single complex multiplet.

Sheng et al. [10] have described a version of the fitting procedure which uses these one-bond cross peaks as the templates. Such an approach is certainly attractive as *all* of the data needed to determine a value for the long-range coupling constant can be obtained from a single experiment. In addition, there is likely to be less overlap of the multiplets than in the simple proton spectrum. However, there are two difficulties with using these one-bond cross peaks. The first is that for a typical value of Δ of around 50 to 100 ms, even the modest spread in the values of one-bond couplings results in a large variation in the intensity of the cross peaks. Indeed, it is quite common for a significant number of the possible one-bond cross peaks to be absent. The second difficulty is that the one-bond cross peaks may overlap the long-range cross peaks, making it impossible to use either for data fitting.

It would therefore be desirable to modify the HMBC experiment so that the one-bond cross peaks have reliable intensities, and so that the two types of cross peaks can be separated. The latter aim can be achieved using the MBOB method developed by Schulte-Herbrüggen et al. [11]. First, we will describe the basis of this method and then go on to describe how a similar approach can be used to achieve more reliable intensities for the one-bond cross peaks.

4.1   *Separating one-bond and long-range cross peaks*

[Fig. 5 about here.]

The way in which the MBOB method works can be understood by referring to Fig. 5. The thick and thin solid lines show how the amplitude of the one-bond cross peaks vary with the preparation delay, Δ, for two different values of the one-bond coupling constant; the rapid modulation is a result of the large coupling constant. The grey line shows a similar curve for the much smaller long-range coupling; in contrast, rather than an oscillation we just see a steady rise. All the curves are plots of the function $\sin(\pi J \Delta)$ — all that is different

is the size of the coupling constant, J.

Consider recording two experiments with the preparation delays indicated by a and a', separated by $1/(^1J_{CH})$. Due to the properties of the sine wave, the amplitudes of the one-bond cross peaks in these two experiments will be *equal* and *opposite*. Thus, if the two experiments are added together, the one-bond cross peaks will cancel. In contrast, the amplitude of the long-range cross peaks for these delays a and a' are both positive and more or less the same; adding the two experiments together will reinforce these cross peaks. On the other hand, if the two experiments are subtracted, the one-bond cross peaks will be retained and the long-range cross peaks will more or less cancel. With this approach, separate one-bond and long-range spectra can be obtained from the same two data sets.

Figure 1 (c) shows how Schulte-Herbrüggen et al. implement this idea by introducing a mobile ^{13}C $180°$ pulse at the start of the sequence. The preparation delay Δ is extended by a time Δ_0 and the extra $180°$ pulse is placed during Δ_0 and at a time τ_f after the start of the sequence; τ_f can vary between zero and Δ_0.

For this simplest MBOB experiment (called a first-order filter) Δ_0 is set to $1/(2\,^1J_{CH})$ a delay which, for compatibility with the subsequent discussion, we will call τ_1. Two separate experiments are recorded for each value of t_1: in the first $\tau_f = \tau_1 = 1/(2\,^1J_{CH})$; in the second $\tau_f = 0$.

When $\tau_f = 0$ the C–H coupling evolves for the whole time $(\Delta + \tau_1)$. When $\tau_f = \tau_1$, the $180°$ pulse forms a spin echo which refocuses the evolution of the coupling at a time $2\tau_1$ after the start of the sequence; thus the C–H coupling evolves for time $(\Delta - \tau_1)$. The effective time for which the coupling evolves in the two experiments thus differs by $2\tau_1$ which, as $\tau_1 = 1/(2\,^1J_{CH})$, is the required difference of $1/(^1J_{CH})$. The advantage of varying the effective preparation delay in this way is that the proton offsets and the proton–proton couplings evolve for time $(\Delta + \tau_1)$ in both cases.

Expressed mathematically, the amplitudes of the cross-peaks in the two experiments vary as a function of the preparation delay in the following ways:

$$\text{Expt. 1}\;:\;\sin\left(\pi J(\Delta - \tau_1)\right) \qquad \text{Expt. 2}\;:\;\sin\left(\pi J(\Delta + \tau_1)\right) \tag{8}$$

where Expt. 1 and Expt. 2 correspond to $\tau_f = \tau_1$ and $\tau_f = 0$, respectively. The sum and difference of these two can be written, using some elementary trigonometry, as:

$$\text{Sum} = \text{Expt. 1} + \text{Expt. 2} = 2\sin\left(\pi J\Delta\right)\cos\left(\pi J\tau_1\right)$$
$$\text{Difference} = \text{Expt. 1} - \text{Expt. 2} = -2\cos\left(\pi J\Delta\right)\sin\left(\pi J\tau_1\right). \tag{9}$$

For the long-range cross peaks, $(\pi J \tau_1)$ is a very small angle so $\cos(\pi J \tau_1) \approx 1$ and $\sin(\pi J \tau_1) \approx 0$. As a result, the long-range cross peaks appear only in the sum spectrum. For the one-bond cross peaks, $(\pi J \tau_1)$ is approximately $(\pi/2)$, so $\cos(\pi J \tau_1) \approx 0$ and $\sin(\pi J \tau_1) \approx 1$. As a result, the one-bond cross peaks appear only in the difference spectrum.

The separation is not perfect in part due to the range of values taken by the one-bond C–H coupling making it necessary to choose a compromise value of τ_1. Schulte-Herbrüggen et al. show that the separation can be improved by constructing higher-order MBOB filters. For example, a second-order filter involves recording four experiments in which the delay τ_f takes the successive values $(0, \tau_1, \tau_2, \tau_1 + \tau_2)$, and where the delay Δ_0 is $(\tau_1 + \tau_2)$. The values of τ_1 and τ_2 are given by

$$\tau_1 = \frac{1}{2[{}^1J_{\text{CH,min}} + 0.146({}^1J_{\text{CH,max}} - {}^1J_{\text{CH,min}})]} \tag{10}$$

$$\tau_2 = \frac{1}{2[{}^1J_{\text{CH,max}} - 0.146({}^1J_{\text{CH,max}} - {}^1J_{\text{CH,min}})]}, \tag{11}$$

where ${}^1J_{\text{CH,min}}$ and ${}^1J_{\text{CH,max}}$ are the lower and upper bounds of the expected range of one-bond coupling constants. The sum of all four experiments contains just the long-range cross peaks, whereas the one-bond correlations appear in the combination of experiments $(1 - 2 - 3 + 4)$.

4.2   Generating more reliable intensities for one-bond cross peaks

The problem with the intensities of the one-bond cross-peaks is illustrated clearly by Fig. 5. It would be quite possible to choose accidentally a preparation delay which resulted in zero (or close to zero) intensity for a particular one-bond cross peak. Of course, a small change in the delay would result in this cross-peak gaining significant intensity, but then another cross-peak arising from a different value of the one-bond C–H coupling constant might have zero intensity. In general, there is no way of choosing a value of the preparation delay such that all one-bond cross peaks will appear with significant intensity.

The broadband MBOB experiment [11] involves adding together, in absolute value mode, experiments recorded using different values of the preparation delay, and so the one-bond cross peaks are present with reliable intensities. However, such an approach is not suitable for our purposes as phase-sensitive data is needed by the fitting procedures.

Our solution to the problem of generating reliable intensities for one-bond cross peaks uses an approach similar to the MBOB filter. Two experiments

are recorded with values of the preparation delay which differ by $1/(2\,^1J_{CH})$. Suppose the two delays correspond to b and b', shown in Fig. 5. For a one-bond coupling constant of 135 Hz, shown by the thick solid line, the amplitude is positive when the delay is b and negative when the delay is b'. Thus, we would obtain greater overall amplitude by *subtracting* the two experiments. On the other hand, for a one-bond coupling constant of 125 Hz, shown by the thin solid line, the amplitudes are positive at both b and b', so the appropriate action would be to add the two experiments together.

In general, as the value of the one-bond coupling is unknown, we cannot determine in advance whether to add or subtract the two spectra. Rather, both combinations are computed, and then the most intense cross peaks are selected from one or the other. To determine the separation of times b and b' we use an average value of the one-bond coupling constant, as in the first-order MBOB filter.

The experimental implementation of this approach is the same as for the MBOB experiment, Fig. 1 (c). However, for the present purpose, the extra delay Δ_0 needs to be $1/(4\,^1J_{CH})$; to avoid confusion with the previous section we will call this delay τ_0. Two experiments are recorded, one with $\tau_f = \tau_0$ and one with $\tau_f = 0$. Thus, in the two experiments the C–H coupling evolves for $(\Delta - \tau_0)$ and $(\Delta + \tau_0)$, respectively.

Following the same analysis as before, the amplitudes of the one-bond cross peaks in the sum and difference of the two experiments are

$$\text{Sum} = 2\sin\left(\pi\,^1J_{CH}\Delta\right)\cos\left(\pi\,^1J_{CH}\tau_0\right)$$
$$\text{Difference} = -2\cos\left(\pi\,^1J_{CH}\Delta\right)\sin\left(\pi\,^1J_{CH}\tau_0\right). \tag{12}$$

As $\tau_0 = 1/(4\,^1J_{CH})$, $\cos\left(\pi\,^1J_{CH}\tau_0\right)$ and $\sin\left(\pi\,^1J_{CH}\tau_0\right)$ are both $1/\sqrt{2}$:

$$\text{Sum} = \sqrt{2}\,\sin\left(\pi\,^1J_{CH}\Delta\right)$$
$$\text{Difference} = -\sqrt{2}\,\cos\left(\pi\,^1J_{CH}\Delta\right). \tag{13}$$

As was mentioned above, whether the sum or difference has the greater signal depends on the precise values of the one-bond coupling and the preparation delay, Δ. However, the key point is that this approach *guarantees* that all of the one-bond cross peaks will appear in either the sum or the difference spectrum with reasonable intensities.

4.3 Combining the two approaches

The separation of the one-bond and long-range cross peaks by a first-order MBOB filter can be achieved at the same time as generating more reliable intensities for the one-bond cross peaks by recording four separate experiments in which the C–H coupling is allowed to evolve for the effective times, Δ_{eff}, given in the following Table 1.

Table 1
Values of Δ_{eff} and τ_{f} needed for a first-order MBOB filter, together with more reliable intensities for one-bond cross peaks, in the modified HMBC sequence of Fig. 1 (d)

experiment	Δ_{eff}	τ_{f}
1	$\Delta + \tau_0 + \tau_1$	0
2	$\Delta - \tau_0 + \tau_1$	τ_0
3	$\Delta + \tau_0 - \tau_1$	τ_1
4	$\Delta - \tau_0 - \tau_1$	$\tau_0 + \tau_1$

As before, $\tau_0 = 1/(4\,^1J_{\text{CH}})$ and $\tau_1 = 1/(2\,^1J_{\text{CH}})$. These four experiments can be achieved experimentally using the pulse sequence shown in Fig. 1 (d) with the value of the delay τ_{f} from the table and with Δ_0 set to $(\tau_0 + \tau_1)$.

The combination $(1 + 2 + 3 + 4)$ can be shown to have the following variation of cross-peak intensity

$$4 \sin\left(\pi J \Delta\right) \cos\left(\pi J \tau_0\right) \cos\left(\pi J \tau_1\right). \tag{14}$$

This is the combination in which, on account of the last term, the one-bond cross-peaks are suppressed. The long-range peaks are present at full intensity as, for small couplings, the last two terms are both very close to one.

There are two combinations in which the long-range cross peaks are suppressed. The combination $(1 + 2 - 3 - 4)$ has the following variation of cross-peak intensity

$$4 \cos\left(\pi J \Delta\right) \cos\left(\pi J \tau_0\right) \sin\left(\pi J \tau_1\right), \tag{15}$$

whereas the combination $(1 - 2 - 3 + 4)$ has the following variation

$$4 \sin\left(\pi J \Delta\right) \sin\left(\pi J \tau_0\right) \sin\left(\pi J \tau_1\right). \tag{16}$$

13

These two combinations have little intensity from the long-range cross-peaks on account of the $\sin(\pi J\tau_1)$ and $\sin(\pi J\tau_0)$ terms. As before, which experiment has the greatest intensity for the one-bond cross peaks depends on the exact values of the one-bond coupling and the delay Δ.

[Fig. 6 about here.]

The separation of the long-range and one-bond cross peaks can be improved by using a second-order MBOB filter. If this is combined with our method for giving more reliable intensities for the one-bond cross peaks, a total of eight separate experiments have to be recorded with the values of τ_f given in Table 2; Δ_0 is set to $(\tau_0 + \tau_1 + \tau_2)$.

Table 2
Values of Δ_{eff} and τ_f needed for a second-order MBOB filter, together with more reliable intensities for one-bond cross peaks, in the modified HMBC sequence of Fig. 1 (d)

experiment	τ_f	experiment	τ_f
1	0	5	τ_0
2	τ_1	6	$\tau_0 + \tau_1$
3	τ_2	7	$\tau_0 + \tau_2$
4	$\tau_1 + \tau_2$	8	$\tau_0 + \tau_1 + \tau_2$

The sum of all eight experiments gives a spectrum in which only the long-range cross peaks are present. The other two combinations which contain only the one-bond cross peaks are : $(1 - 2 - 3 + 4 + 5 - 6 - 7 + 8)$, the intensity in which depends on $\sin(\pi J\Delta)$, and $(1 - 2 - 3 + 4 - 5 + 6 + 7 - 8)$, the intensity in which depends on $\cos(\pi J\Delta)$.

Figure 6 shows spectra of strychnine recorded using this approach. The spectra demonstrate both the clean separation of long-range and one-bond cross peaks which can be obtained, and the different intensities of the cross peaks in the two combinations (b) and (c) in which only one-bond cross peaks appear.

5 Fitting using one-bond templates

As has been mentioned earlier, multiplets from the one-bond cross peak can be used as templates in the fitting procedure so as to obtain estimates of the long-range couplings. There are two ways to proceed: the first, originally described by Sheng et al. [10], is to use one half of the one-bond cross peak as a template; the second, described here for the first time, is to use the *whole* cross peak as a template.

The two halves of the one-bond cross peak are separated by $^1J_{\mathrm{CH}}$, which is much greater than the typical width of a proton multiplet. We might therefore expect that the two halves can be separated cleanly from one another. This is the case if the multiplet is in absorption mode, but in HMBC spectra the multiplets are in anything but absorption mode. When dispersion contributions are present, significant overlap between the two sides of the one-bond cross peak can be seen, as shown by the fact that the baseline between them does not return to zero (see, for example, Fig. 10 (a)). In such circumstances an entirely clean separation of the two halves is not possible and this is why it may be preferable to use the entire one-bond cross peak.

5.1 Fitting using one half of the one-bond cross peak: Method II

Both halves of the one-bond cross peak already have the necessary phase modulation due to the evolution of proton offsets and proton–proton couplings during the preparation delay. So, all that we need to do is excise one side or the other, and then shift it by half of the one-bond coupling so that the excised multiplet is centred at the proton shift. Then the anti-phase coupling is introduced to create the trial multiplet which can be compared to the HMBC multiplet, just as before. Shifting the multiplet by half of the one-bond coupling is performed in the time-domain.

[Fig. 7 about here.]

The overall fitting process can be described in the following way and is also illustrated in Fig. 7. The time-domain signal corresponding to a one-bond cross peak can be written

$$S_{\mathrm{one-bond}}(t_2) = A_{\mathrm{one-bond}} \times S_{\mathrm{proton}}(t_2 + \Delta) \times \sin\left(\pi\,^1J_{\mathrm{CH}}t_2\right). \qquad (17)$$

The final term is the one which gives rise to the large anti-phase splitting by the one-bond coupling, $^1J_{\mathrm{CH}}$.

In order to separate out the two sides of the multiplet we write the sine in terms of exponentials:

$$\sin\left(\pi\,^1J_{\mathrm{CH}}t_2\right) = \frac{1}{2\mathrm{i}}\left[\exp\left(\mathrm{i}\pi\,^1J_{\mathrm{CH}}t_2\right) - \exp\left(-\mathrm{i}\pi\,^1J_{\mathrm{CH}}t_2\right)\right]. \qquad (18)$$

Selecting the right or left part of the multiplet involves selecting just one of these terms; arbitrarily we shall select the first one. Then the time domain signal becomes

15

$$S_{\text{half one-bond}}(t_2) = \frac{1}{2i} \, A_{\text{one-bond}} \times S_{\text{proton}}(t_2 + \Delta) \times \exp\left(i\pi \, ^1J_{\text{CH}}t_2\right). \quad (19)$$

The shift required to centre the multiplet at the proton offset is $(-\pi \, ^1J_{\text{CH}})$ rad s^{-1}; this is achieved in the time domain by multiplying by $\exp\left(-i\pi \, ^1J_{\text{trial}}t_2\right)$. We have allowed for the fact that we may not know the value of the actual one-bond coupling, so will need to use a trial value, $^1J_{\text{trial}}$.

The final step is to introduce the anti-phase long-range coupling by multiplying by $\sin\left(\pi J_{\text{trial}}t_2\right)$ and, as before, introducing an amplitude factor:

$$
\begin{aligned}
S_{\text{trial}}(t_2) = \, & A_{\text{trial}} \times S_{\text{half one-bond}}(t_2) \\
& \times \sin\left(\pi J_{\text{trial}}t_2\right) \times \exp\left(-i\pi \, ^1J_{\text{trial}}t_2\right) \\
= \, & \frac{1}{2i} \, A_{\text{trial}} \, A_{\text{one-bond}} \times S_{\text{proton}}(t_2 + \Delta) \times \sin\left(\pi J_{\text{trial}}t_2\right) \\
& \times \exp\left(i\pi \, ^1J_{\text{CH}}t_2\right) \times \exp\left(-i\pi \, ^1J_{\text{trial}}t_2\right). \quad (20)
\end{aligned}
$$

This function for the trial multiplet is compared with that for the long-range cross peak (Eq. 1) in a least-squares fitting procedure. The parameters to be adjusted are the trial amplitude, the trial long-range coupling and the trial one-bond coupling. In practice, we have found that it is sufficient to estimate the one-bond coupling from the spectrum and then just use this value for $^1J_{\text{trial}}$ without further adjustment.

[Fig. 8 about here.]

Figure 8 shows this version of the fitting procedure in action for the C8–H13 cross peak in strychnine. As before, with the correct choice of parameters, the trial multiplet is an excellent fit for the long-range cross-peak multiplet.

5.2   Fitting using the entire one-bond cross peak: Method III

The second way of using the one-bond cross peak involves using the *whole* cross peak, rather than just half of it. In contrast to the previous case, both the one-bond and long-range cross peaks are manipulated.

[Fig. 9 about here.]

The fitting procedure involves splitting the long-range multiplet by a trial anti-phase one-bond coupling, $^1J_{\text{trial}}$, and splitting the *whole* one-bond cross peak by a trial anti-phase long-range coupling, J_{trial}. The two resulting multiplets are then compared in a least-squares fitting procedure with the overall

16

amplitude and the two trial couplings being the adjustable parameters. The whole process is illustrated in Fig. 9.

The fitting process can be described mathematically in the following way. The long-range multiplet is described by the function $S_{\text{HMBC}}(t_2)$ in Eq. 1; this function is multiplied by $\sin(\pi\,^1J_{\text{trial}}t_2)$ to generate the large anti-phase splitting

$$
\begin{aligned}
S'_{\text{HMBC}}(t_2) &= S_{\text{HMBC}}(t_2) \times \sin\left(\pi\,^1J_{\text{trial}}t_2\right) \\
&= A_{\text{HMBC}} \times S_{\text{proton}}(t_2 + \Delta) \\
&\quad \times \sin\left(\pi J_{\text{CH}}t_2\right) \times \sin\left(\pi\,^1J_{\text{trial}}t_2\right).
\end{aligned}
\tag{21}
$$

The one-bond multiplet is described by the function $S_{\text{one-bond}}(t_2)$ of Eq. 17. This function is multiplied by $\sin(\pi J_{\text{trial}}t_2)$, to generate the small anti-phase splitting; a trial amplitude is also included

$$
\begin{aligned}
S'_{\text{one-bond}}(t_2) &= A_{\text{trial}} \times S_{\text{one-bond}}(t_2) \times \sin\left(\pi J_{\text{trial}}t_2\right) \\
&= A_{\text{trial}}\, A_{\text{one-bond}} \times S_{\text{proton}}(t_2 + \Delta) \\
&\quad \times \sin\left(\pi\,^1J_{\text{CH}}t_2\right) \times \sin\left(\pi J_{\text{trial}}t_2\right).
\end{aligned}
\tag{22}
$$

We now see that provided the parameters A_{trial}, J_{trial} and $^1J_{\text{trial}}$ have the appropriate values, $S'_{\text{HMBC}}(t_2)$ and $S'_{\text{one-bond}}(t_2)$ are identical. The optimum values of these parameters are found in a least-squares fitting procedure, as described above. As before, we have found it sufficient to estimate $^1J_{\text{trial}}$ from the spectrum and then leave this parameter fixed.

[Fig. 10 about here.]

Figure 10 shows this version of the fitting procedure in action for the C8–H13 cross peak in strychnine. As before, with the correct choice of parameters, the two manipulated multiplets are in close agreement.

5.3 Isotope shifts

When using one-bond cross peaks as templates in the fitting process, it is important to recognise that a one-bond and a long-range cross peak involving the *same* proton may not be centred at precisely the same offset in F_2. This is because when the proton is directly attached to a ^{13}C atom, as it is in the molecules which lead to the one-bond cross peak, its chemical shift may be slightly different to the case where the same proton is attached to a ^{12}C

17

atom, as it is for molecules which lead to the long-range cross peak. This small difference is called an *isotope shift*.

The presence of this isotope shift means that the trial multiplet will never quite match the HMBC multiplet no matter what values of the trial amplitude and coupling are used. However, it is a simple matter to shift the offset of the trial multiplet by multiplying it in the time domain by $\exp{(i\epsilon t_2)}$, where ϵ is a trial shift which may be positive or negative. This shift simply becomes another parameter in the least-squares fitting procedure, and so its value is optimised along with the values of the other parameters. Typically, we have found that incorporating this shift significantly improves the fit between the trial and HMBC multiplets. Shifts of up to 1 Hz are not uncommon.

It should be noted that in fitting method II, which uses half of the one-bond cross peak, introducing this parameter to allow for isotope shifts is identical to allowing variations in the value of the trial one-bond coupling.

The contour maps of χ^2 as a function of A_{trial} and J_{trial} shown in Figs. 8 and 10 are constructed using estimated values of the one-bond coupling and zero isotope shift. The position of the minimum in these plots does not necessarily correspond, therefore, to the position of the minimum which will be found when all of the parameters are allowed to vary. For example, in the case of Fig. 10, the χ^2 plot shows a minimum at $J_{\mathrm{trial}} = 7.0$ Hz, but when the isotope shift is allowed to vary, the Levenberg–Marquardt algorithm finds the minimum to be at 6.4 Hz.

6 A one-dimensional experiment

From a two-dimensional HMBC experiment we should be able to measure a value for the coupling constant from the majority of the cross peaks. Having such complete data from one experiment is an advantage, but there may be occasions when only a small part of the data is actually required — for example, where a question of stereochemistry can be resolved by measuring just one long-range coupling. In such situations, a selective one-dimensional version of the HMBC experiment may well be an attractive option as it can be recorded quickly and conveniently.

A large number of such selective experiments have been proposed over the years [12]. For our present purposes, the main requirement is that the fitting procedure developed for the two-dimensional HMBC can be applied to data from the one-dimensional experiment. A pulse sequence which satisfies this requirement is shown in Fig. 1 (e).

This sequence is essentially an HMBC experiment in which t_1 has been replaced by a selective echo on ^{13}C; only long-range couplings to the carbon (or carbons) which experience the selective 180° pulse will give rise to observable signals. All other signals are suppressed effectively by the two gradients which flank the selective pulse. The proton offset and proton–proton couplings evolve for the total time $(\Delta + 2\delta + t_{\mathrm{sel}})$, where the time periods are defined in Fig. 1 (e).

Ideally, one would like to decouple the protons during the selective pulse to ^{13}C. However, we have found it difficult to achieve this without at the same time disrupting severely the evolution of the proton magnetization. In principle, it should be possible to minimize this effect by applying *complete* cycles of a cyclic decoupling sequence such as WALTZ-16 [13]; we have had limited success with such an approach.

Since the selective pulse is applied to the proton-coupled ^{13}C spectrum, the bandwidth of the pulse must be set to encompass a multiplet split by the large one-bond C–H coupling, unless it is a quaternary carbon which is being excited. It is possible to set the selective pulse to excite part of the multiplet (e.g. half of a doublet), although this will result in a loss of intensity.

The selective pulse is on resonance for the ^{13}C of interest, so it is not necessary to be concerned about the evolution of the offset. However, the pulse itself may give rise to a phase shift and this in turn will lead to a phase shift of the observed proton multiplet; clearly such a phase shift must be avoided as its presence would invalidate the fitting procedure. Our experience has been that with modern spectrometers, which are generally capable of attenuating the radio-frequency power level without introducing significant phase shifts, no problems associated with the phase of this selective pulse were found. If such phase errors are a problem, then a solution would be to use a double echo [14].

[Fig. 11 about here.]

Figure 11 shows three multiplets all arising from long-range correlations between H8, H23b and H23a to C12 in strychnine. Spectrum (a) was obtained using the one-dimensional pulse sequence of Fig. 1 (f) whereas (b) was obtained using the modified HMBC sequence of Fig. 1 (e). The data show that, as is required, the one-dimensional experiment produces essentially identical multiplets to those found in the two-dimensional HMBC. The multiplets from the one-dimensional experiment can therefore be analysed in exactly the same way as those from the two-dimensional experiment.

19

Table 3. Values of long-range C–H couplings (in Hz) in strychnine determined using different fitting procedures

C label	H label[a]	method I	method III	method II	literature
15	13	3.5	3.4		6.6[c]
14		4.6	4.7		4.7[c]
8		6.3	6.4	6.3	
12		0.6	0.8		1.2[b]
21		7.8	7.5		7.4[b]
14	15b	3.2	3.6		4.8[c]
13		3.3	3.5		3.8[b], 4.6[c]
16		2.7	3.0		
21		6.0	6.0		6.1[b]
7	17	3.2	†	3.1	3.2[c]
16/8		5.6	5.5		
6		1.9	†	1.8	
14	15a	1.8	2.8	2.8	3.2[c]
13		8.0	8.1		7.9[c],7.7[b]
7		7.2	7.3		7.3[c]
16		4.5	4.3		
12		0.9	2.3	2.1	
21		0.9	1.4		1.9[b]
12	11b	7.0	6.9		7.1[b]
10		7.9	7.9		7.4[b]
14	20b	5.4	5.3		5.5[c]
18		3.5	3.1	3.4	3.6[c]
16		6.9	6.9		
22		4.5	4.6		
21		2.4	1.0	1.0	
17	18b	5.6	5.1		4.9[c]
20		7.1	7.1		7.4[c]
13	11a	3.4[d]	3.3		
12		2.5[d]	0.8	0.8	1.7[b]
10		5.8[d]	6.5	5.6	6.4[b]
17	18a	2.7	3.2	3.5	2.4[c]
7		4.6	5.2		5.2[c]
16		†	4.3		
18	20a	9.3	9.6	9.5	9.5[c]
22		6.1	5.8		
21		4.9	4.6		
17	8	5.9	5.9		5.9[c]
7		2.5	2.4		2.6[c]
12		5.5	5.6		5.4[b]
6		3.7	3.7		
5		3.2	3.1		
12	23a	5.6	5.7		
22		3.8	4.0		
21		3.3	3.2		
12	23b	8.6	8.2		
22		4.0	3.9		
21		8.5	8.3		
8	12	5.8	5.9	5.8	
23		2.4	6.8	2.4	
10		†	†	5.8	
14	22	7.9	8.5	8.6	8.9[c]
20		4.9	5.6	5.1	12.5[c], 5.7[b]
23		5.7	7.1	7.1	6.2[b]
2	4	7.5	7.4		
6		5.5	5.5		
5		0.9	0.8		

[a]diastereotopic pairs labelled according to reference [15]. [b]average value of results quoted in reference [16]. [c]taken from reference [15]. [d]template taken from TOCSY spectrum. †analysis failed to converge to a satisfactory result.

7   Results and discussion

Table 3 presents values for long-range couplings in strychnine which have been measured using method I (taking the template from the proton spectrum) and method III (using the whole one-bond cross peak as the template); a smaller number of couplings have also been measured using method II (using half the one-bond cross-peak as the template). Where they are available, the values of these couplings reported in the literature are also given.

Generally speaking, for couplings greater than about 2.5 Hz, there is good agreement between the values derived from the three methods; we can thus have confidence in all of these methods. For smaller couplings, there tend to be significant differences between the values determined by the different methods. Such small couplings give rise to weaker cross peaks and, in addition, the anti-phase splitting starts to become comparable with the linewidth. As a result, the minimum in the χ^2 map becomes shallower so that the precise location of the minimum itself is more easily perturbed by noise or experimental imperfections; this is what accounts for the variation in the results given by the different methods. For this data set, which is typical of what one might expect, we conclude that it would be unwise to interpret, in a quantitative way, any values below approximately 2.5 Hz. This limit can be lowered by improving the signal-to-noise ratio (for example, by increasing Δ) and, if possible, the resolution.

The shape of the χ^2 map is also influenced by the form of the HMBC multiplet. For example, multiplets which have complex structures, such as that shown in Fig. 4 (b), tend to give χ^2 maps in which there is a single well-defined minimum. We can understand this by realizing that it is only when the value of the trial coupling is correct that all of the details will match between the HMBC and trial multiplet. On the other hand, if the HMBC multiplet is rather featureless, the minimum in the χ^2 map is less well defined and so the resulting value of the coupling is less reliable.

[Fig. 12 about here.]

Occasionally, the χ^2 plot does not show one well-defined minimum, such as those seen in Figs. 4, 8 and 10. For example, fitting the C10–H12 cross peak using method I gives the χ^2 plot shown in Fig. 12. The global minimum is at $J_{\text{trial}} \approx 0.5$ Hz, but there are subsidiary minima at 5.8 Hz and 10.5 Hz. Given the intensity of the cross-peak, it is inconceivable that the coupling can be as small as 0.5 Hz, so despite this corresponding to the global minimum, we are forced to reject the value.

If the trial multiplets are inspected by eye it is found that for $J_{\text{trial}} = 0.5$ Hz there is quite close agreement with the HMBC multiplet, but that the fit does

21

not appear to be so good when $J_{\text{trial}} = 5.8$ Hz. A further check is provided by comparing the C10–H12 cross peak with the C8–H12 cross peak. For the latter, the fitting procedure straightforwardly gives a value of around 5.8 Hz for the long-range coupling. However, this cross peak has little resemblance to the C10–H12 cross peak; this casts doubt on the C10–H12 coupling being 5.8 Hz as indicated by the subsidiary minimum in the χ^2 plot. The lesson to be drawn from this discussion is that when multiple minima are present, caution is needed in interpreting the results of the fitting procedure.

In general, our conclusions about these fitting procedures are that: (1) reasonably large values of the coupling constant determined by the fitting procedures are reliable, but that small values need to be treated with caution; (2) it is useful to fit a given cross peak using more than one method – the resulting spread of values gives some indication of reliability; (3) the χ^2 plot should be checked for the presence of multiple minima as these may be an indication of poor reliability.

Marquez et al. [16] have recently reviewed the large number of methods which have been proposed for measuring long-range C–H couplings. Most of these methods are based on HMQC- or HSQC-type correlation experiments which have been modified to manipulate the way in which either or both the proton-proton couplings and the long-range C–H coupling appear in the multiplets. The general aim is to achieve a multiplet from which a splitting can be identified as the long-range C–H coupling. In this way, the need for any kind of fitting procedure, such as that described here, is obviated. However, this is achieved at the expense of more complex pulse sequences and possible compromises in the sensitivity of the experiment.

The procedure proposed in this paper relies on the use of a fitting procedure, and so the data analysis is inherently more complex than simply measuring a splitting from a multiplet. In addition, the fitting procedure requires extra data, but we have shown that by utilizing the one-bond cross peaks this extra data can be acquired at the same time as the HMBC spectrum. The pulse sequences are not complex and involve no compromises. Thus, the approach suggested here represents a straightforward and efficient way of measuring values for long-range C-H couplings.

Acknowledgements

References

[1] A. Bax, M. Summers, ^{1}H and ^{13}C assignments from sensitivity-enhanced detection of heteronuclear multiple-bond connectivity by 2D multiple quantum NMR, J. Am. Chem. Soc. 108 (1986) 2093–2094.

[2] J. J. Titman, D. Neuhaus, J. Keeler, Measurement of long-range heteronuclear coupling constants, J. Magn. Reson. 85 (1989) 111–131.

[3] L. Braunschweiler, R. R. Ernst, Coherence transfer by isotropic mixing: application to proton correlation spectroscopy, J. Magn. Reson. 53 (1983) 521–528.

[4] M. J. Thrippleton, J. Keeler, Elimination of zero-quantum interference in two-dimensional NMR spectra, Angew. Chem., Int. Ed. Engl. 00 (2003) 00–00.

[5] R. N. Bracewell, The Fourier transform and its applications, McGraw-Hill international book company, London, 1978.

[6] D. O. Cicero, G. Barbato, R. Bazzo, Sensitivity enhancement of a two-dimensional experiment for the measurement of heteronuclear long-range coupling constants, by a new scheme of coherence slection by gradients., J. Magn. Reson. 148 (2001) 209–213.

[7] J. Ruiz-Cabello, G. W. Vuister, C. T. W. Moonen, P. van Gelderen, J. S. Cohen, P. C. M. van Zijl, Gradient-enhanced heteronuclear correlation spectroscopy - theory and experimental aspects, J. Magn. Reson. 100 (1992) 282–302.

[8] G. Zhu, D. A. Torcia, A. Bax, Discrete Fourier transformation of NMR signals. The relationship between sampling delay time and spectral baseline, J. Magn. Reson. Ser. A 105 (1993) 219–222.

[9] W. H. Press, S. A. Teukolsky, W. T. Vetterling, B. P. Flannery, Numerical recipes in C: the art of scientific computing, Cambridge University Press, Cambridge, 1996.

[10] S. Sheng, H. van Halbeek, Accurate and precise measurement of heteronuclear long-range couplings by a gradient-enhanced two-dimensional multiple-bond correlation experiment, J. Magn. Reson. 130 (1998) 296–299.

[11] T. Schulte-Herbrüggen, A. Meissner, A. Papanikos, M. Meldal, O. W. Sørensen, Optimising delays in the MBOB, broadband HMBC, and broadband XLOC NMR pulse sequences, J. Magn. Reson. 156 (2002) 282–294.

[12] T. Parella, High-quality 1D spectra by implementing pulsed-field gradients as the coherence pathway selection procedure, Magn. Reson. Chem. 34 (1996) 329–347.

[13] A. J. Shaka, J. Keeler, T. Frenkiel, R. Freeman, An improved sequence for broadband decoupling: WALTZ-16, J. Magn. Reson. 52 (1983) 335–338.

[14] K. Stott, J. Stonehouse, T. L. Hwang, J. Keeler, A. J. Shaka, Excitation sculpting in high-resolution NMR spectroscopy – application to selective NOE experiments, J. Am. Chem. Soc. 117 (1995) 4199–4200.

[15] V. Blechta, F. del Río-Portilla, R. Freeman, Long-range carbon–proton couplings in strychnine, Magn. Reson. Chem. 32 (1994) 134–137.

[16] B. L. Márquez, W. H. Gerwick, R. T. Wiliamson, Survey of NMR experiments for the determination of ^{n}J(C,H) heteronuclear coupling constants in small molecules, Magn. Reson. Chem. 39 (2001) 499–530.
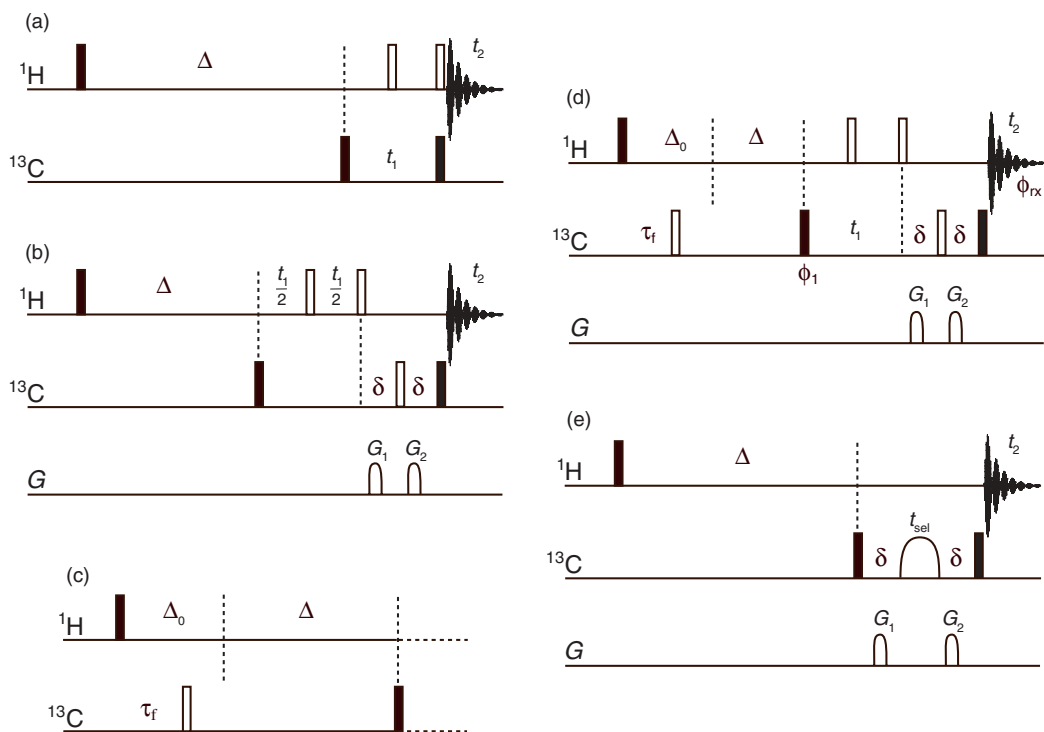
Fig. 1. Pulse sequences for different variants of the basic HMBC experiment. Radiofrequency pulses applied to proton and carbon are shown on the lines marked ^{1}H and ^{13}C, respectively; filled rectangles indicate 90° pulses, and open rectangles indicate 180° pulses. Pulse field gradients are shown in the line marked G. Sequence (a) is the conventional HMBC experiment, except that an extra proton 180° pulse is included at the end of t_1; see text for details. Sequence (b) is a gradient-selected HMBC experiment which has been designed specifically to produce multiplets with the same phase properties as those from sequence (a). The delays δ are included simply to accommodate the gradient pulses G_1 and G_2. Sequence (c) shows how evolution of the C–H coupling can be affected by the placement of an extra ^{13}C 180° pulse at the start of the sequence; see text for details. Sequence (d) is a new HMBC-type experiment which makes is possible to separate long-range from one-bond correlations, and also results in more even intensities for the one-bond cross peaks. As described in the text, several data sets are recorded with different values of τ_f and then recombined to give the required spectra. In sequence (d) the phases are as follows: $\phi_1 = (x, -x)$ and $\phi_{rx} = (x, -x)$; all other pulses are phase x. Sequence (e) is a one-dimensional (selective) version of the HMBC experiment; the experiment is designed to give multiplets with identical phase properties to those from sequences (a), (b) and (d). The selective element is a 180° pulse, duration t_{sel}, flanked by the two gradients.
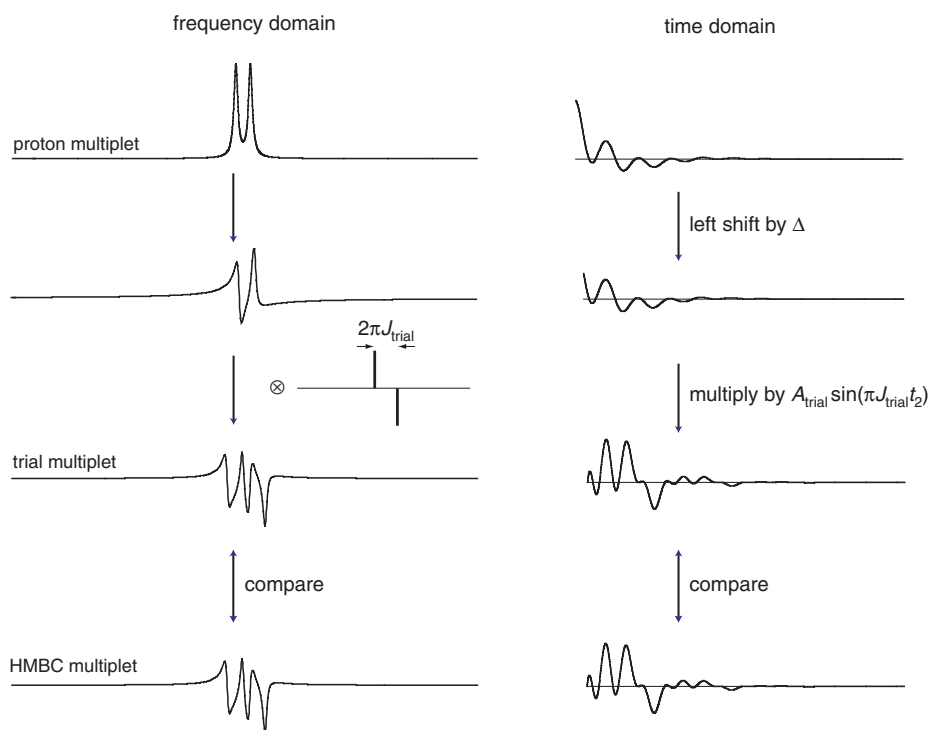
Fig. 2. The basic fitting procedure (method I), described in detail in the text, can be envisaged in either the frequency domain (shown on the left) or time domain (shown on the right). At the top is the conventional absorption-mode proton multiplet. The first step is to introduce the phase modulation due to the preparation delay, Δ, in the HMBC sequence; it is convenient to do this by left shifting the time-domain signal by a number of data points corresponding to the delay Δ. Next, the anti-phase splitting is introduced: in the frequency domain this is achieved by convoluting (represented by $\otimes$) the proton multiplet with an "anti-phase stick multiplet" formed from two delta-functions separated by $2\pi J_{\text{trial}}$ rad s^{-1}; in the time domain the same effect is achieved by multiplication by $A_{\text{trial}} \sin(\pi J_{\text{trial}} t_2)$. These two steps generate a trial multiplet which can then be compared with the multiplet from the HMBC spectrum; the two parameters A_{trial} and J_{trial} are adjusted in a least-squares fitting procedure in order to obtain the best fit between the trial and HMBC multiplets. In the diagram the trial multiplet has been constructed using the values of these two parameters which give the best fit. Note that the time- and frequency-domain signals are both complex, but that only the real parts are plotted here.
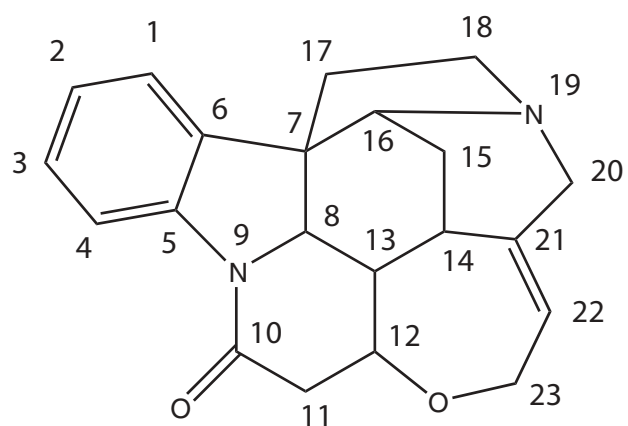
Fig. 3. The structure of strychnine, showing the numbering convention used.
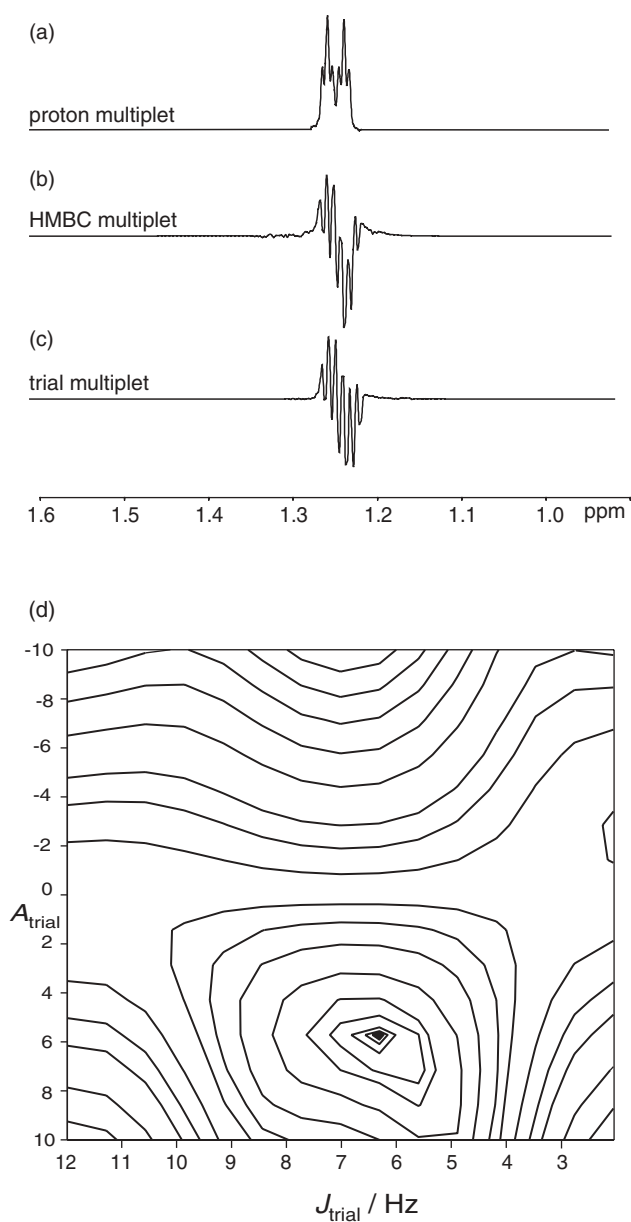
Fig. 4. Experimental data showing application of the fitting procedure (method I) to the strychnine C8–H13 cross-peak multiplet. The H13 multiplet shown in (a) was excised from the conventional proton spectrum; the multiplet in (b) was excised from a cross section, taken parallel to F_2, of the HMBC spectrum, through the C8–H13 cross peak. Shown in (c) is the best-fit trial multiplet constructed as described in the text; the agreement with (b) is excellent. Shown in (d) is a contour plot of χ^2 (in arbitrary units), as defined in Eq. 5, as a function of the two parameters A_{trial} and J_{trial}. The minimum is clearly visible at $J_{\text{trial}} = 6.3$ Hz.
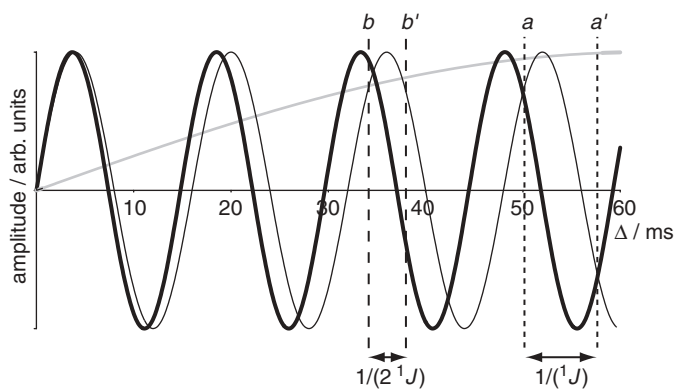
Fig. 5. Plot showing how the amplitude of one-bond and long-range cross peaks varies with the preparation delay, Δ. The thick and thin solid lines shows how the amplitude of one-bond cross peaks vary for couplings of 135 Hz and 125 Hz, respectively. The grey line shows the slower variation which is characteristic of the very much smaller long-range coupling (here 8 Hz). The significance of the times labelled a, a', ... is explained in the text.
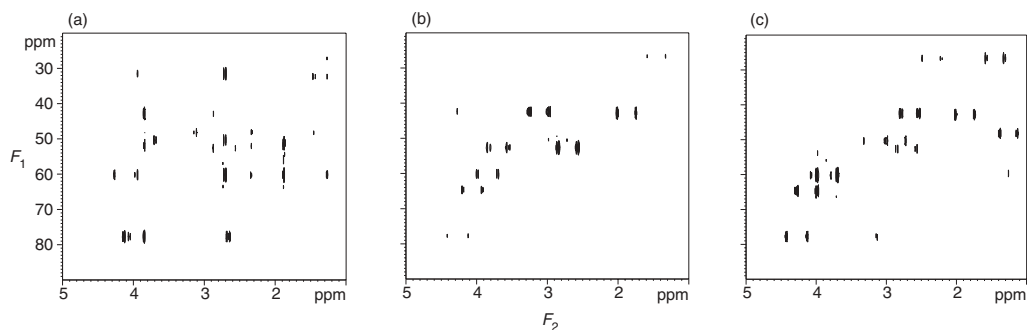
Fig. 6. Part of the HMBC spectra of strychnine showing the clean separation of long-range and one-bond cross peaks, and the more reliable intensities of the latter, which can be obtained using the new method proposed here. Spectrum (a) is the sum of the eight separate experiments, recorded using the pulse sequence of Fig. 1 (d) and the values of τ_f given in Table 2; only long-range cross peaks are present. Spectra (b) and (c) are the two combinations (of the eight experiments) which contain just the one-bond cross peaks; the different intensities of particular cross peaks in the two spectra are clearly visible. For each of the eight separate experiments, t_1 was incremented in 128 steps to a maximum value of 5.7 ms, and 8 transients were recorded for each t_1 value. The acquisition time was 0.8 s, and the recycle delay between experiments was 2.5 s. The delays Δ, τ_0, τ_1 and τ_2 were 51.2, 1.750, 3.073 and 3.928 ms, respectively; Δ_0 was therefore 8.751 ms. The gradients G_1 and G_2 were of duration 1.95 ms, of Gaussian shape and truncated at the 1% level; their amplitudes were set to -29.75% and 49.75% (of the full intensity of 40 G cm^{-1}) for the P-type and -49.75% and 29.75% for the N-type spectrum. The delay δ was 2 ms. Spectra were recorded at 500 MHz for proton, the total experiment time was 13 hours and the sample concentration was approximately 120 mM in CDCl$_3$.
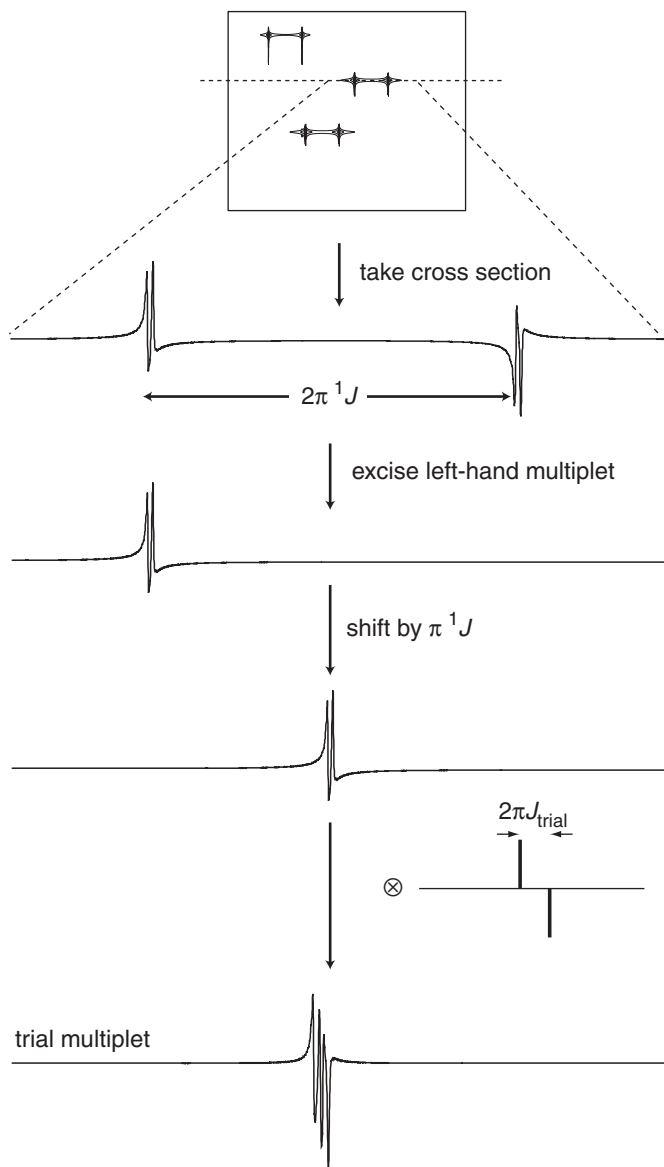
30

Fig. 7. Illustration of a method, introduced by Sheng et al. [10], by which a one-bond bond cross peak can be used to generate a trial multiplet; we term this approach method II. First, a cross section containing the one-bond multiplet is taken from the two-dimensional spectrum; note that the phase modulation due to the evolution of proton shifts and couplings is already present. Then, one half of the multiplet is excised (here the left-hand side) and shifted to the right by half the one-bond coupling; this centres the multiplet at the proton offset. Finally, the shifted multiplet is convoluted with an anti-phase stick multiplet (as in Fig. 2) so as to introduce the trial anti-phase coupling.

31
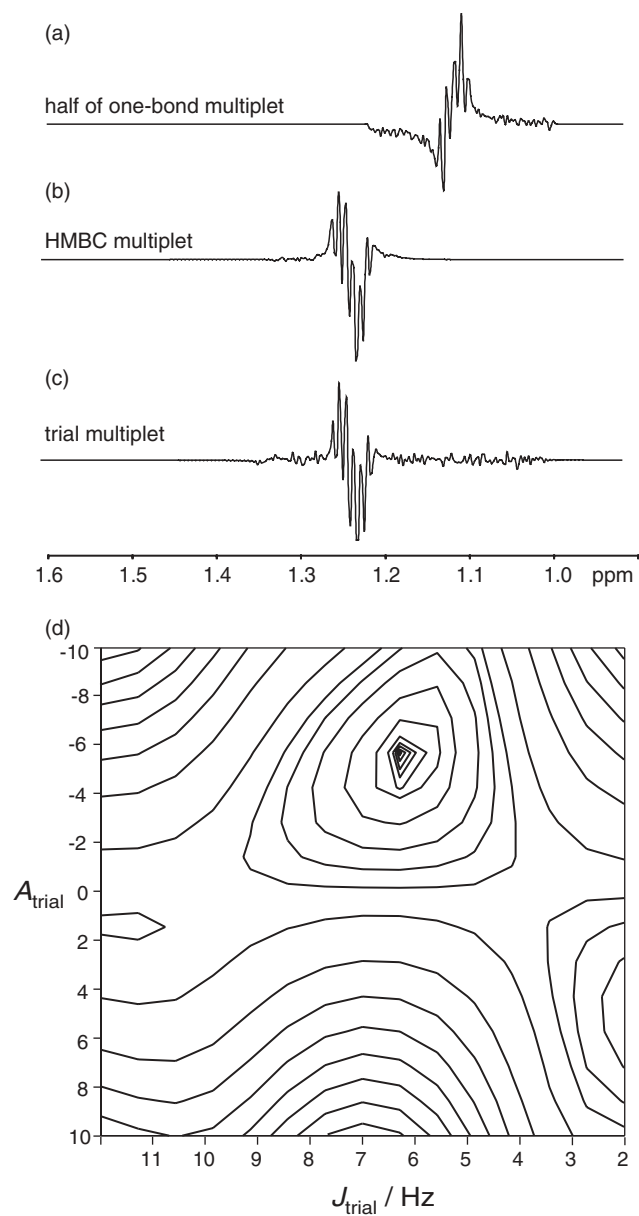
Fig. 8. Experimental data showing method II being used to determine the value of the long-range C–H coupling from the C8–H13 cross-peak multiplet in strychnine. In contrast to Fig. 4, rather than using a multiplet from the proton spectrum, half of the one-bond cross peak is used to construct the trial multiplet. Spectrum (a) shows the right-hand half of the one-bond cross peak (i.e. that between C13 and H13) which has been excised from a cross-section through the modified HMBC spectrum. Spectrum (b) shows the HMBC (long-range) multiplet which is to be fitted, and (c) shows the best fit trial multiplet constructed from (a); the agreement between (b) and (c) is excellent. Also shown is a plot of χ^2 as a function of the two parameters A_{trial} and J_{trial}; to compute this plot $^1J_{\text{trial}}$ is set to 125 Hz and the trial isotope shift, ϵ, is set to zero.
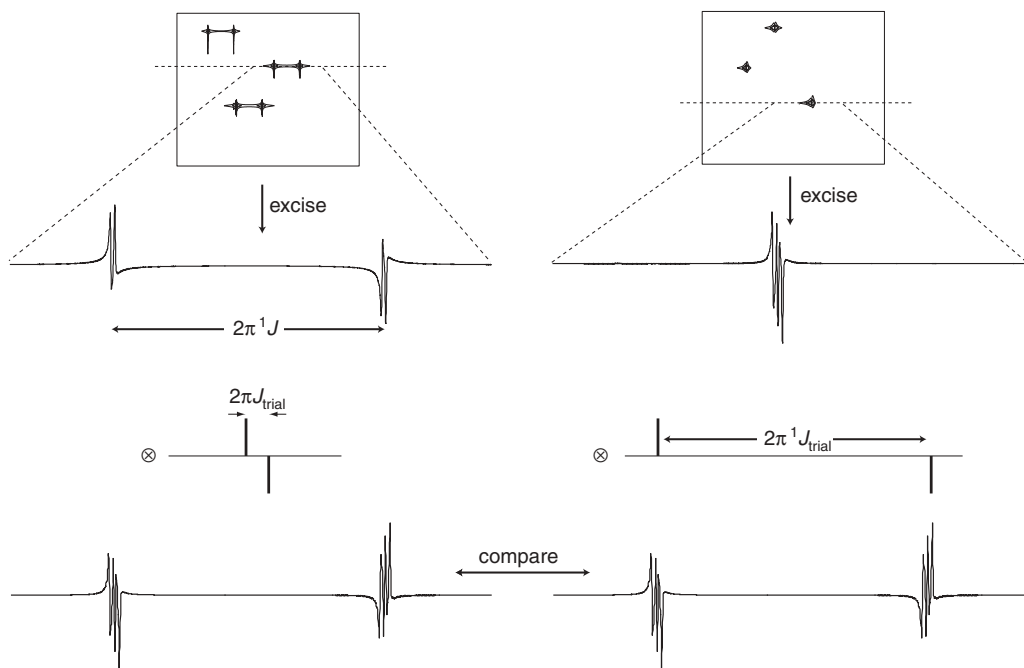
32

Fig. 9. Illustration of fitting method III in which a one-bond cross peak is used to generate a trial multiplet. On the left are shown the manipulations which are applied to the whole one-bond cross peak. First the multiplet is excised from a suitable cross-section from the two-dimensional spectrum. Then, the trial anti-phase long-range coupling is introduced, as before, by convolution. On the right are shown the manipulations which are applied to the long-range cross peak. The multiplet is excised and then the one-bond coupling is introduced. The resulting multiplets at the bottom on the left and the right can now be compared and the best-fit values of J_{trial}, $^{1}J_{\mathrm{trial}}$ and A_{trial} found.
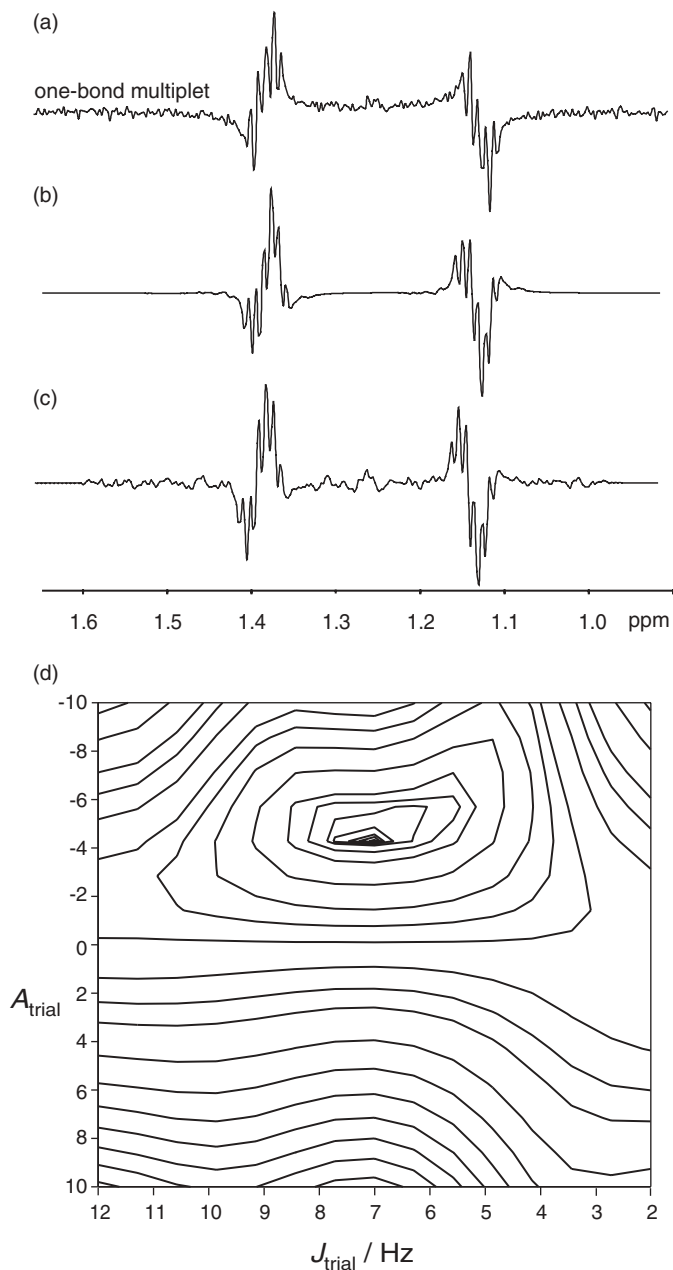
Fig. 10. Experimental data showing fitting method III being used on the C8–H13 cross-peak multiplet from strychnine. In contrast to Fig. 8, rather than using one side of the one-bond cross-peak multiplet, the whole multiplet is used. Spectrum (a) shows the complete one-bond multiplet and spectrum (b) is the long-range multiplet into which the one-bond anti-phase coupling has been introduced. Spectrum (c) shows the effect of introducing the anti-phase splitting due to the long-range coupling into the multiplet shown in (a). At the optimum value of the long-range coupling (used here to construct (c)), there is excellent agreement between (b) and (c). Also shown is a plot of χ^2 as a function of the two parameters A_{trial} and J_{trial}; to compute this plot $^{1}J_{\text{trial}}$ is set to 125 Hz and the trial isotope shift, ϵ, is set to zero.
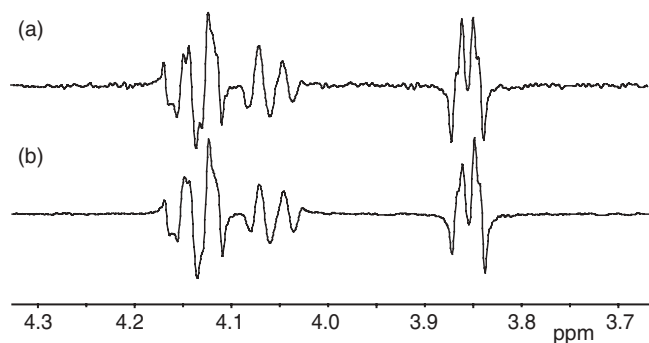
34

Fig. 11. Cross-peak multiplets arising from long-range correlations to C12 in strychnine. Spectrum (a) was obtained using the one-dimensional pulse sequence of Fig. 1 (e) whereas (b) was obtained from a two-dimensional HMBC experiment. Note that, as required, the multiplets from the one-dimensional experiment are essentially identical to those from the two-dimensional HMBC. The parameters for the two-dimensional experiment are as in the caption to Fig. 6. For the one-dimensional experiment 1024 transients were recorded using an acquisition time of 0.8 s and a recycle delay between experiments of 1 s. The delays Δ and δ were 55 and 2 ms, respectively. The gradients G_1 and G_2 were of duration 1.95 ms, of Gaussian shape and truncated at the 1% level; their amplitudes were set to 29.76% and 49.76% (of the full intensity of 40 G cm^{-1}). The selective 180° pulse was of duration 5 ms, of Gaussian shape and truncated at the 1% level. The total experiment time was 31 minutes.
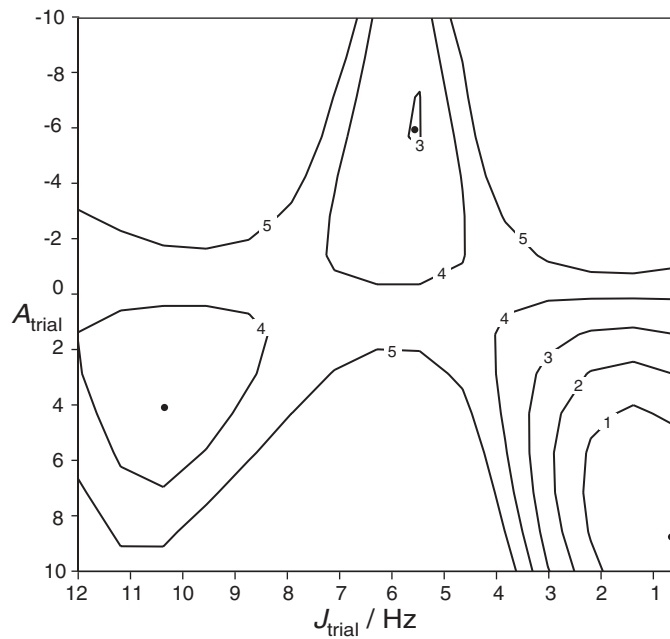
Fig. 12. Contour plot of χ^2 found when fitting the C10–H12 multiplet from strychnine using method I. Contours are plotted at evenly spaced intervals and are labelled 1, 2, … as the level rises. Three minima, indicated by ●, are clearly visible; see text for discussion.